**Supporting Information**

**for**

# Electrochemical synthesis of Palladium-N-heterocyclic carbene (NHC) complexes

*Roman V. Larkovich,* [a] *Francis Bru,* [a] *Maxime R. Vitale,* [b] *Laurence Grimaud,* [b] *and Catherine S.J. Cazin* [*a]

[a] Department of Chemistry and Centre for Sustainable Chemistry, Ghent University, Krijgslaan 281 (S-3), 9000 Ghent, Belgium. E-mail: catherine.cazin@ugent.be

[b] Laboratoire des Biomolécules (LBM), Département de Chimie, Ecole Normale Supérieure, PSL University, Sorbonne Université, CNRS, 75005 Paris, France;

## Contents

## General considerations

$^{1}H$ and $^{13}C$-{$^{1}H$} Nuclear Magnetic Resonance (NMR) spectra were recorded on a Bruker Advance 300 and 400 Ultrashield spectrometers at 298K. Chemical shifts (expressed in parts per million) are referenced to residual solvent peaks: ($CHCl_3$: $\delta_H$ = 7.26 ppm, $\delta_C$ = 77.16 ppm) at 298K in $CDCl_3$. [Pd($\eta^3$-cin)($\mu$-Cl)]$_2$ was used as received. *n*-$Bu_4NBF_4$ was dried at 110 °C for 6 h and then stored under dry nitrogen atmosphere. Acetonitrile was dried over MW-activated 3 Å molecular sieves for 14 h. Other solvents and commercially available reagents were used without preliminary purification. IPr·HCl,[1] IMes·HCl,[1] SIPr·HCl,[2] SIMes·HCl,[2] $IPr^{Cl}$·HCl,[3] BIAN-IMes·HCl,[4] and SIPr(OMe)·HCl[5] were synthesised following corresponding literature procedures.

Elemental analyses were performed at Université de Namur, rue de Bruxelles, 55 B-5000 Namur, Belgium.

All reactions were carried out using an IKA ElectraSyn 2.0 device, a Metrohm Multi Autolab M204 potentiostat or an Origaflex OGF 500 potentiostat. When using a split cell two compartments were separated by an anion exchange membrane – a DuPont Nafion 117 perfluorinated membrane of 430 µm thickness (Aldrich).

Cyclic voltammetry experiments (CV) were performed with a Metrohm Multi Autolab M204 potentiostat connected to a Nova software interface in a three-electrode cell in a glovebox at 25 °C with a scan rate of 0.1 $V \cdot s^{-1}$ using a glassy carbon disk (d = 3 mm) as a working electrode, a platinum wire as a counter electrode and an Ag electrode as a quasi-reference electrode in 10 mL of a 0.1 M solution of n-$Bu_4NPF_6$ in the solvent. Ferrocene was added to the background solution at the end of the experiment to reference recorded peak potentials to the Ag/AgCl/3M KCl reference electrode potential with the ferrocene redox potential $Fc^+$/Fc equal to 0.42 V (vs Ag/AgCl/3M KCl).[6]

**CV studies under different conditions**

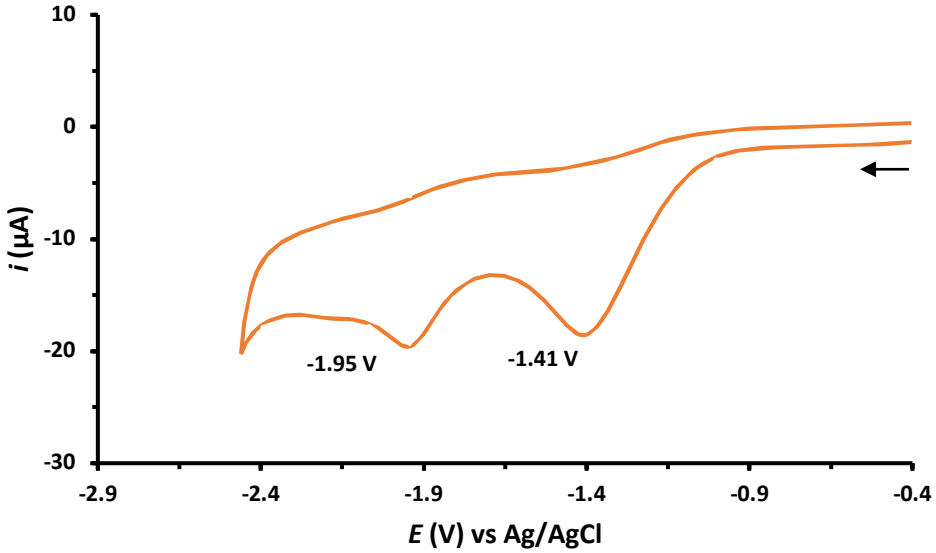


**Figure S1.** CV of [IPrH][Pd($\eta^3$-cin)$Cl_2$] (1 mM) in MeCN (0.1 M *n*-$Bu_4NPF_6$ as a supporting electrolyte) at a glassy carbon disk electrode (d = 3 mm) with a scan rate of 0.1 $Vs^{-1}$ at 25 °C. The CVs were performed towards **reduction** potentials.

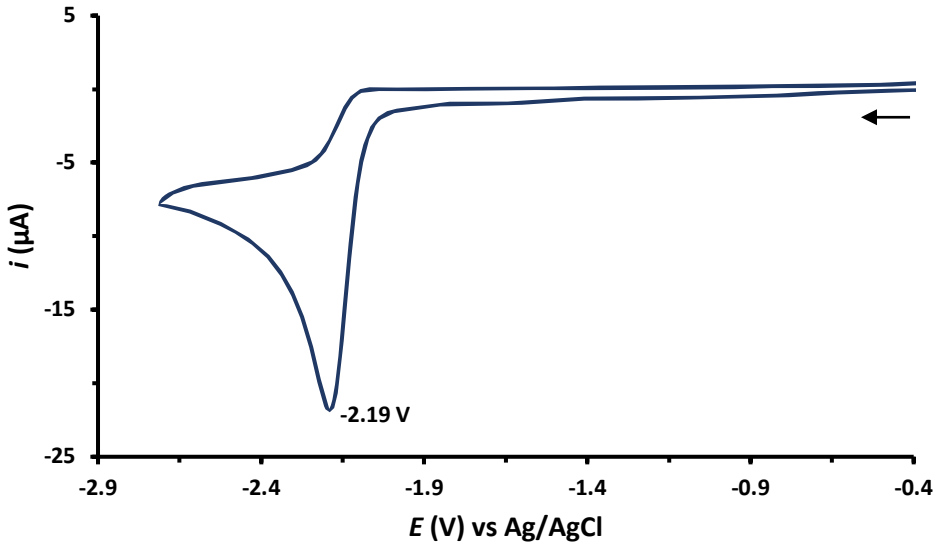


**Figure S2.** CV of IPr·HCl (1 mM) in MeCN (0.1 M *n*-$Bu_4NPF_6$ as a supporting electrolyte) at a glassy carbon disk electrode (d = 3 mm) with a scan rate of 0.1 $Vs^{-1}$ at 25 °C. The CVs were performed towards **reduction** potentials.

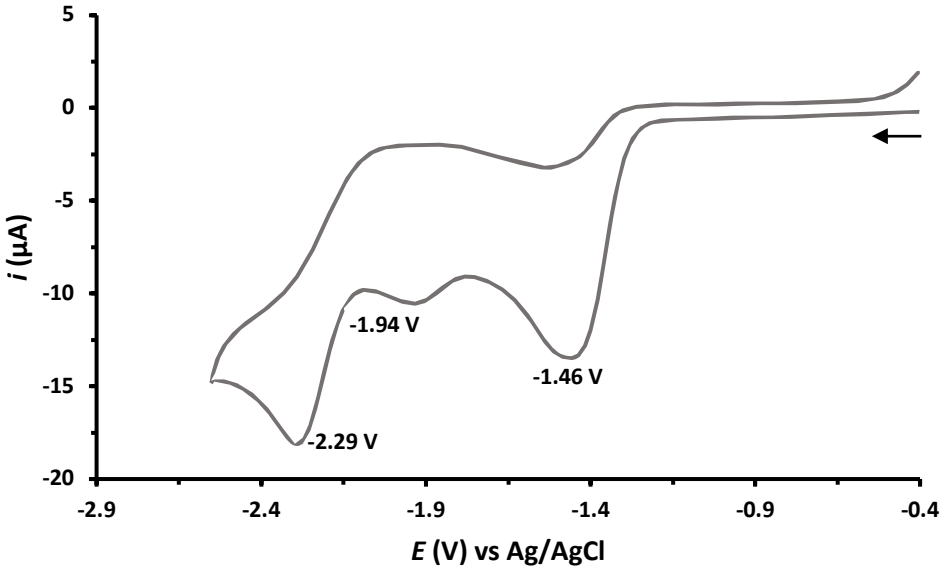


**Figure S3.** CV of [Pd($\eta^3$-cin)(Cl)(IPr)] (1 mM) in MeCN (0.1 M *n*-$Bu_4NPF_6$ as a supporting electrolyte) at a glassy carbon disk electrode (d = 3 mm) with a scan rate of 0.1 $Vs^{-1}$ at 25 °C. The CVs were performed towards **reduction** potentials.

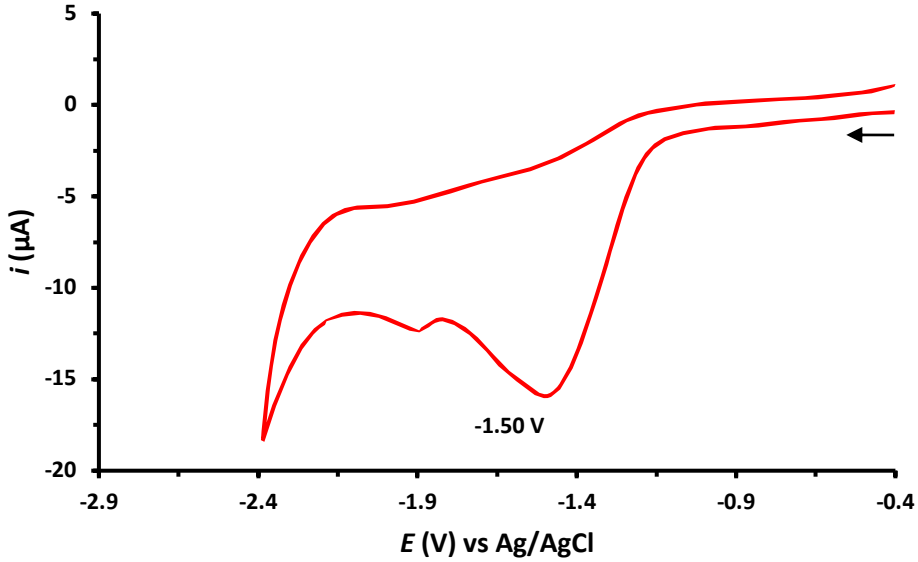


**Figure S4.** CV of [*n*-$Bu_4N$][Pd($\eta^3$-cin)$Cl_2$] (1 mM) in MeCN (0.1 M *n*-$Bu_4NPF_6$ as a supporting electrolyte) at a glassy carbon disk electrode (d = 3 mm) with a scan rate of 0.1 $Vs^{-1}$ at 25 °C. The CVs were performed towards **reduction** potentials.

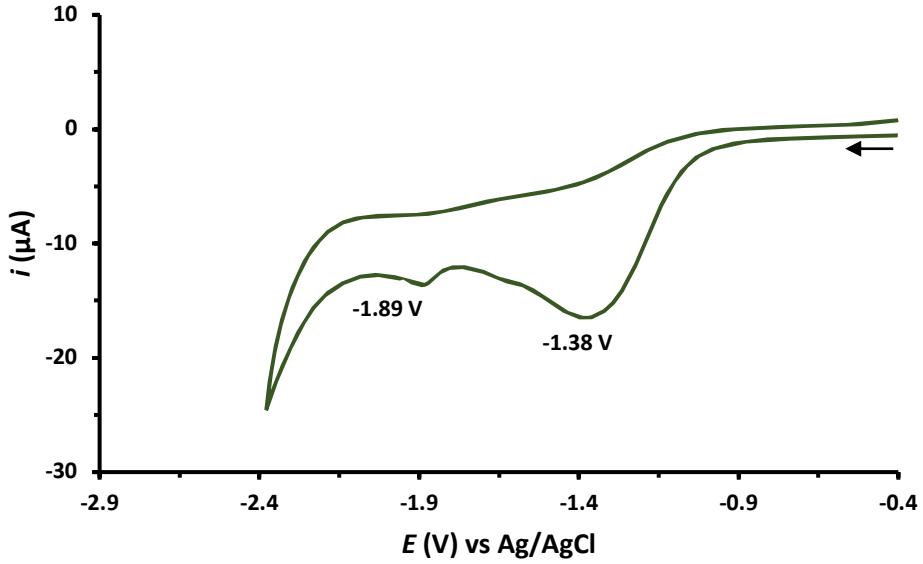


**Figure S5.** CV of [Pd($\eta^3$-cin)($\mu$-Cl)]$_2$ (0.5 mM) in MeCN (0.1 M *n*-Bu$_4$NPF$_6$ as a supporting electrolyte) at a glassy carbon disk electrode (d = 3 mm) with a scan rate of 0.1 Vs$^{-1}$ at 25 °C. The CVs were performed towards **reduction** potentials.

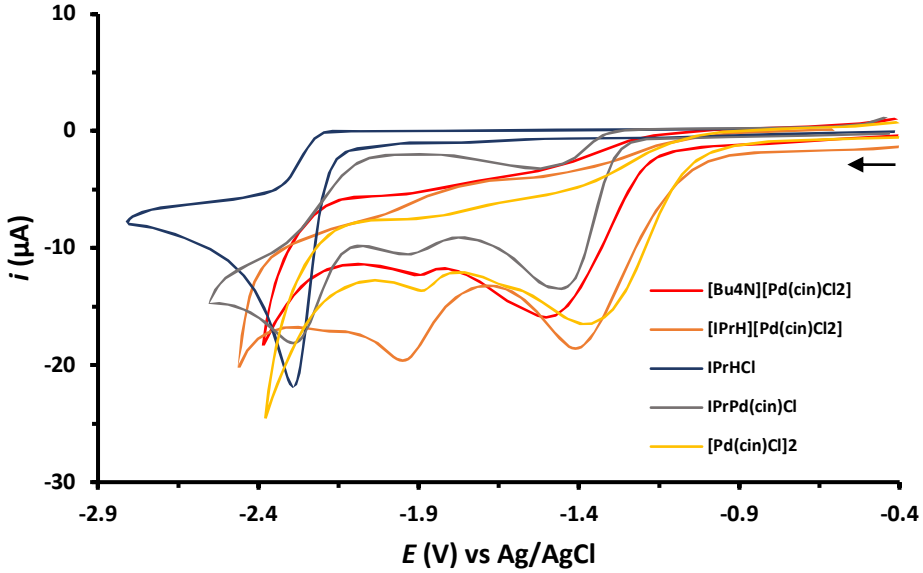


**Figure S6.** The superimposition of the cathodic region of CVs of [IPrH][Pd($\eta^3$-cin)Cl$_2$] (orange); IPr·HCl (blue); [Pd($\eta^3$-cin)(Cl)(IPr)] (gray), [*n*-Bu$_4$N][Pd($\eta^3$-cin)Cl$_2$] (red), [Pd($\eta^3$-cin)($\mu$-Cl)]$_2$ (green). Other conditions: a glassy carbon working electrode (d = 3 mm), a Pt counter electrode, scan rate = 0.1 Vs$^{-1}$, and a 0.1 M *n*-Bu$_4$NPF$_6$ electrolyte. The CVs were performed towards **reduction** potentials.

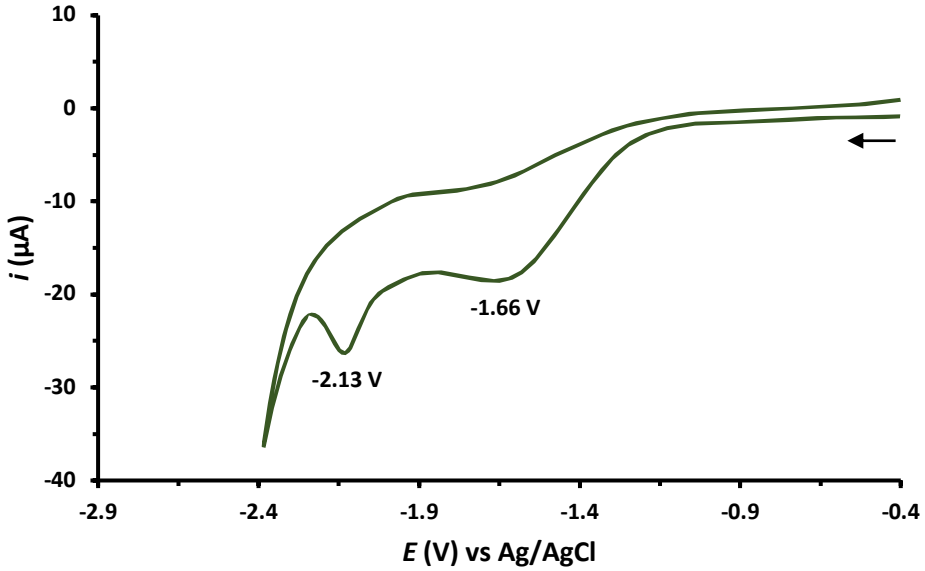


**Figure S7.** CV of [IPrH][Pd($\eta^3$-allyl)$Cl_2$] (1 mM) in MeCN (0.1 M *n*-$Bu_4NPF_6$ as a supporting electrolyte) at a glassy carbon disk electrode (d = 3 mm) with a scan rate of 0.1 $Vs^{-1}$ at 25 °C. The CVs were performed towards **reduction** potentials.]

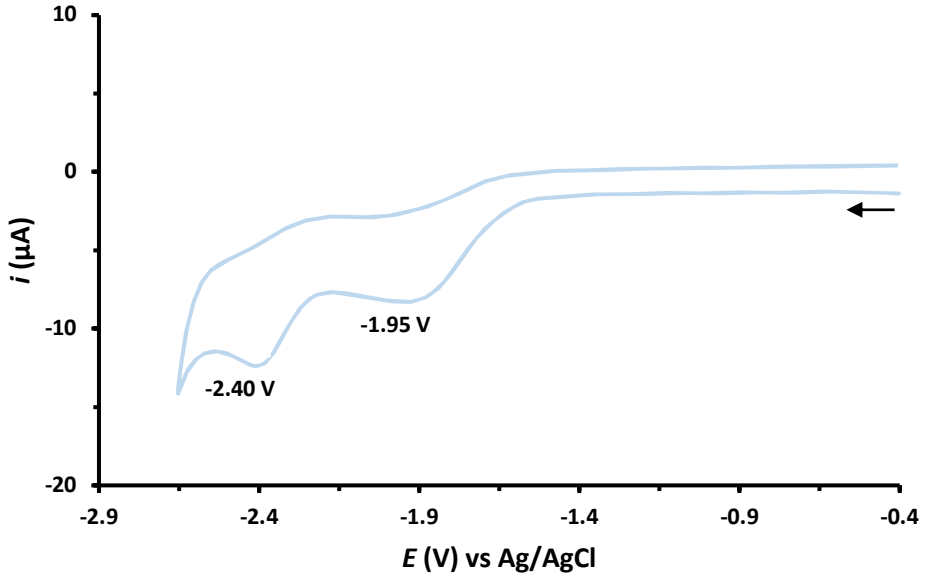


**Figure S8.** CV of [Pd($\eta^3$-allyl)(Cl)(IPr)] (1 mM) in MeCN (0.1 M *n*-$Bu_4NPF_6$ as a supporting electrolyte) at a glassy carbon disk electrode (d = 3 mm) with a scan rate of 0.1 $Vs^{-1}$ at 25 °C. The CVs were performed towards **reduction** potentials.

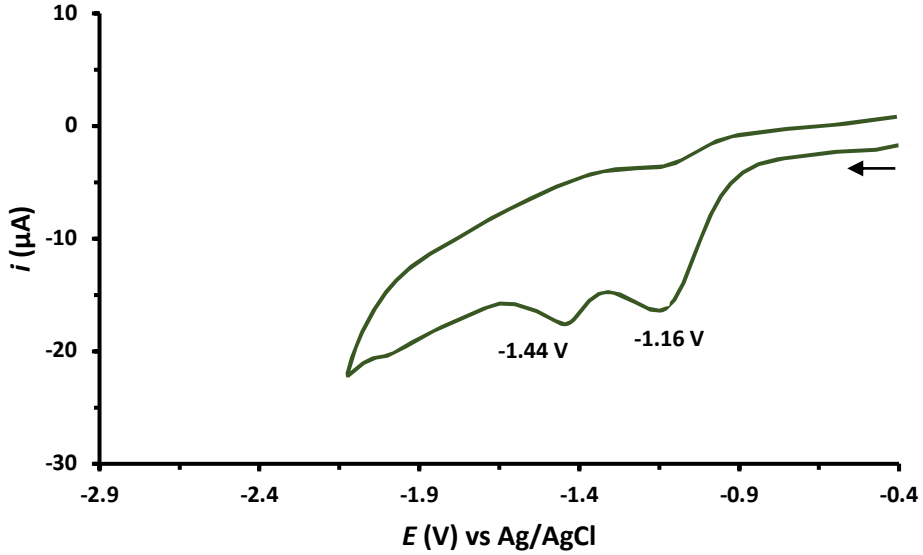


**Figure S9.** CV of [IPrH][Pd(1-$^{t}$Bu-indenyl)$Cl_2$] (1 mM) in MeCN (0.1 M *n*-$Bu_4NPF_6$ as a supporting electrolyte) at a glassy carbon disk electrode (d = 3 mm) with a scan rate of 0.1 $Vs^{-1}$ at 25 °C. The CVs were performed towards **reduction** potentials.

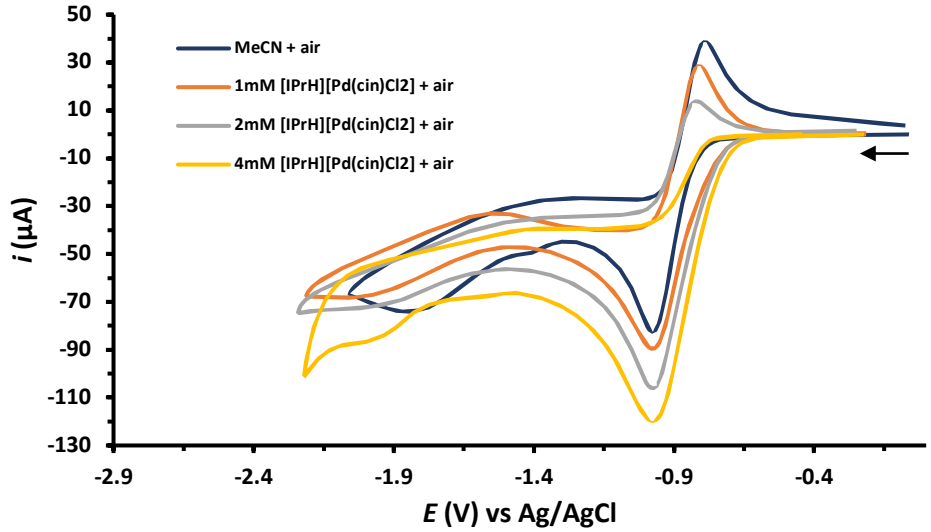


**Figure S10.** CVs of MeCN and [IPrH][Pd($\eta^3$-cin)$Cl_2$] (1, 2, and 4 mM) in MeCN with dissolved oxygen (0.1 M *n*-$Bu_4NPF_6$ as a supporting electrolyte) at a glassy carbon disk electrode (d = 3 mm) with a scan rate of 0.1 $Vs^{-1}$ at 25 °C. The CVs were performed towards **reduction** potentials.

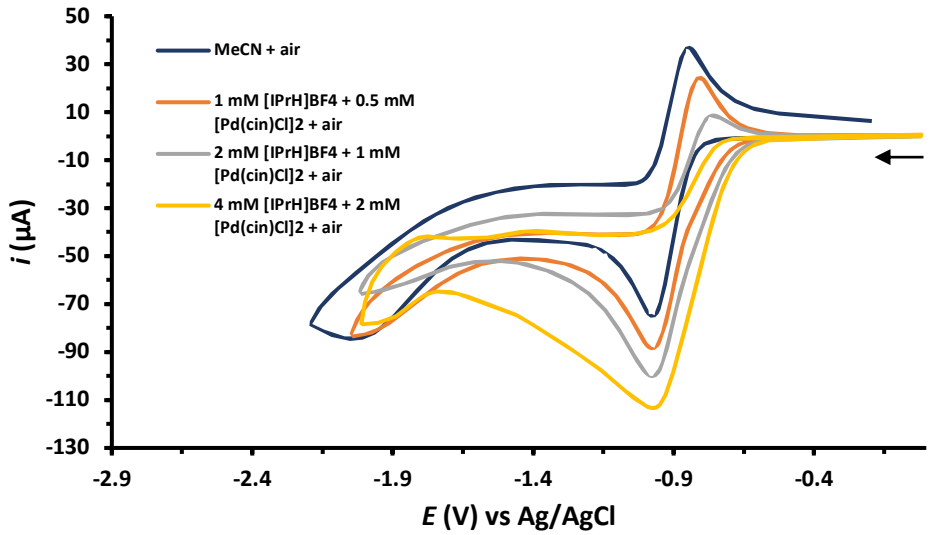


**Figure S11.** CVs of MeCN and {IPr·$HBF_4$ + 0.5 [Pd($\eta^3$-cin)($\mu$-Cl)]$_2$} (1, 2, and 4 mM) in MeCN with dissolved oxygen (0.1 M *n*-$Bu_4NPF_6$ as a supporting electrolyte) at a glassy carbon disk electrode (d = 3 mm) with a scan rate of 0.1 $Vs^{-1}$ at 25 °C. The CVs were performed towards **reduction** potentials.

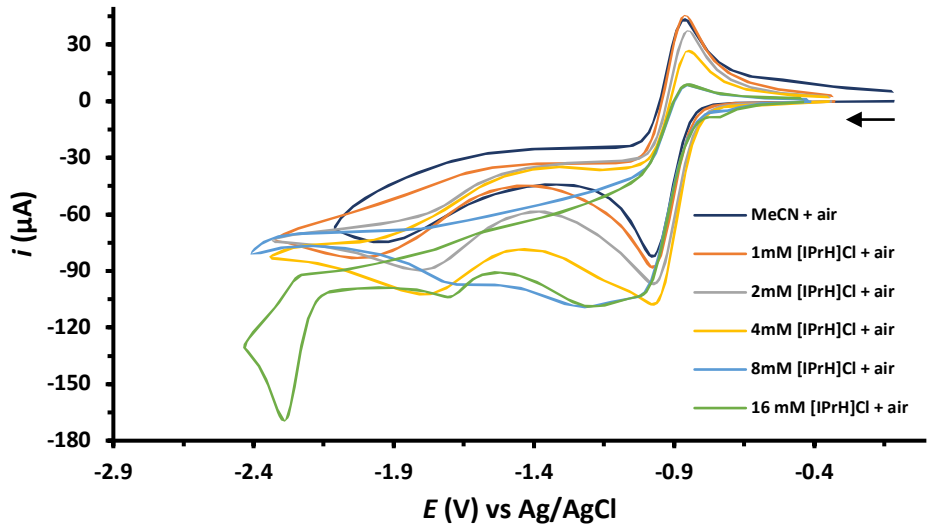


**Figure S12.** CVs of MeCN and IPr·HCl (1, 2, 4, 8, and 16 mM) in MeCN with dissolved oxygen (0.1 M *n*-$Bu_4NPF_6$ as a supporting electrolyte) at a glassy carbon disk electrode (d = 3 mm) with a scan rate of 0.1 $Vs^{-1}$ at 25 °C. The CVs were performed towards **reduction** potentials.

## Optimisation of reaction conditions

Decomposition of the reaction mixture is accompanied by the formation of Pd (black) while an imidazolium cation remains intact in the form of its chloride. In this regard, 2 conversion values are presented: the conversion of Pd species (Conv. Pd, %) and the conversion of an imidazolium cation (Conv. Imid., %).

**Table S1.** Optimisation of reaction conditions - influence of starting material.

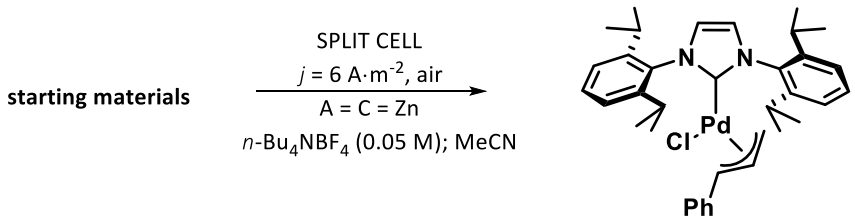


| Entry | Starting material(s) | n (e) (F/mol) | Conv. Pd (Conv. Imid) (%) | Yield[a] (%) | Isolated yield (%) |
|---|---|---|---|---|---|
| 1 | [IPrH][Pd($\eta^3$-cin)$Cl_2$] | 1.0 | 94 (94) | 85 | - |
| 2 | [IPrH][Pd($\eta^3$-cin)$Cl_2$] | 1.6 | 100 (100) | 82 | - |
| 3 | [IPrH][Pd($\eta^3$-cin)$Cl_2$] | 2.1 | 100 (100) | 79 | |
| 4 | IPrHCl + 0.5 [Pd($\eta^3$-cin)($\mu$-Cl)]$_2$ | 1.6 | 100 (100) | 83 | 82 |
| 5 | IPrH$BF_4$ + 0.5 [Pd($\eta^3$-cin)($\mu$-Cl)]$_2$ | 1.0 | 55 (55) | 47 | - |
| 6 | IPrH$BF_4$ + 0.5 [Pd($\eta^3$-cin)($\mu$-Cl)]$_2$ | 1.6 | 100 (88) | 67 | - |
| 7 | IPrH$BF_4$ + 0.5 [Pd($\eta^3$-cin)($\mu$-Cl)]$_2$ | 2.1 | 100 (94) | 63 | - |

[a] Yield determined by NMR using 1,3,5-trimethoxybenzene as internal standard.

**Table S2.** Optimisation of reaction conditions - influence of electrodes setup.

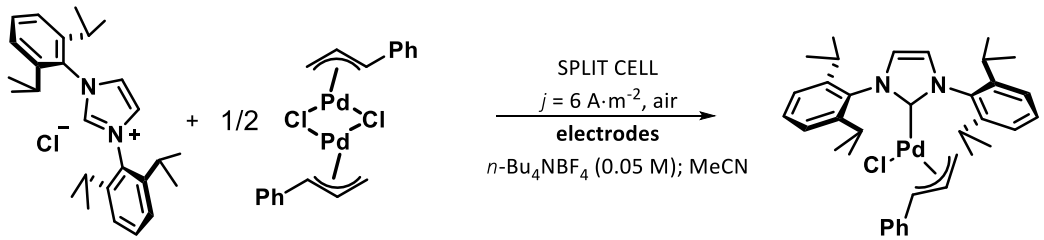


| Entry | Electrodes | n (e) (F/mol) | Conv. Pd (Conv. Imid), (%) | Yield[a] (%) |
|---|---|---|---|---|
| 1[b] | Anode = Cathode = Zn | 1.6 | 100 (100) | 83 |
| 2[b] | Cathode = glassy carbon<br>Anode = Zn | 1.6 | 100 (100) | 74 |

[a] Yield determined by NMR using 1,3,5-trimethoxybenzene as internal standard. [b] Using preformed palladate [IPrH][Pd($\eta^3$-cin)$Cl_2$] instead of the IPr·HCl + ½ [Pd($\eta^3$-cin)($\mu$-Cl)]$_2$ mixture.

**Table S3.** Optimisation of reaction conditions - influence of oxygen presence.

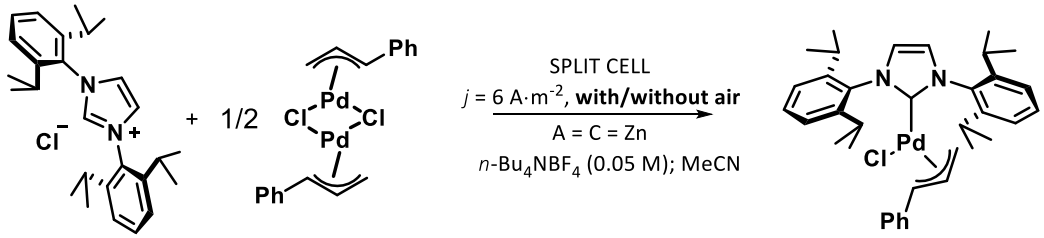


| Entry | Conditions | n (e) (F/mol) | Conv. Pd (Conv. Imid) (%) | Yield[a] (%) |
|---|---|---|---|---|
| 1[c] | Air | 1.6 | 100 (100) | 82 |
| 2[c] | Ar atmosphere (glovebox) | 1.6 | 100 (<5) | <5[b] |
| 3[c] | Air + 1.6 eq. of BHT | 1.6 | 100 (100) | 88 |
| 4[c] | Air + 20 eq. of BHT | 1.6 | 100 (100) | 85 |
| 5[c] | Air + 1.6 eq. of benzoquinone | 1.6 | 100 (100) | 85 |
| 6[c] | Air + 1.6 eq. of TEMPO | 1.6 | 100 (100) | 78 |

[a]Yield determined by NMR using 1,3,5-trimethoxybenzene as internal standard. [b] Reaction accompanied by formation of a substantial amount of Pd black having covered electrodes and precipitated in the bulk solution.[c] Using preformed palladate [IPrH][Pd($\eta^3$-cin)$Cl_2$] instead of the IPr·HCl + ½ [Pd($\eta^3$-cin)($\mu$-Cl)]$_2$ mixture.

**Table S4.** Optimisation of reaction conditions - influence of the supporting electrolyte.

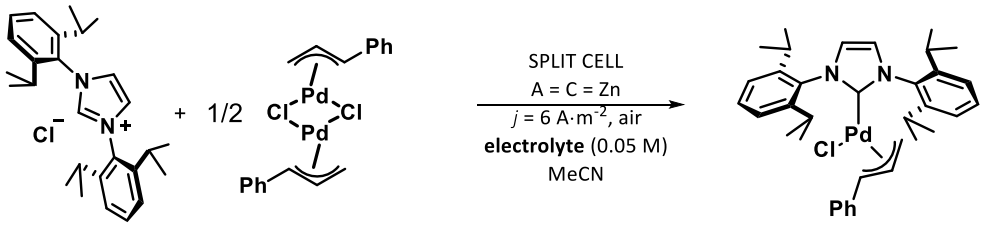


| Entry | Electrolyte | n (e) (F/mol) | Conv. Pd (Conv. Imid) (%) | Yield[a] (%) |
|---|---|---|---|---|
| 1[c] | *n*-$Bu_4NBF_4$ | 1.6 | 100 (100) | 82 |
| 2[c] | $Me_4NBF_4$ | 1.6 | 100 (92) | 61 |
| 3[c] | $Et_4NOTs$ | 1.6 | 100 (78) | 69[b] |
| 4[c] | *n*-$Bu_4NCl$ | 1.6 | 100(100) | 76 |

[a] Yield determined by NMR using 1,3,5-trimethoxybenzene as an internal standard. [b] The solution in the anodic compartment turned turbid, while the electrode was covered with a white layer which subsequently precipitated. [c] Using preformed palladate [IPrH][Pd($\eta^3$-cin)$Cl_2$] instead of the IPr·HCl + ½ [Pd($\eta^3$-cin)($\mu$-Cl)]$_2$ mixture.

**Table S5.** Optimisation of reaction conditions - influence of the constant current value.

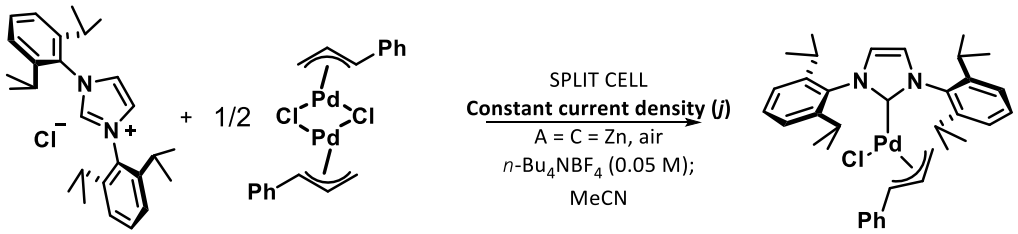


| Entry | Current value (*I*), mA | n (e), F/mol | Conv. Pd (Conv. Imid), % | Yield[a], % |
|---|---|---|---|---|
| 1[b] | 2.5 | 1.6 | 100 (100) | 82 |
| 2[b] | 1 | 1.6 | 100 (91) | 73 |
| 3[b] | 5 | 1.6 | 100 (90) | 75 |

[a] Yield determined by NMR using 1,3,5-trimethoxybenzene as an internal standard. [b] Using preformed palladate [IPrH][Pd($\eta^3$-cin)$Cl_2$] instead of the IPr·HCl + ½ [Pd($\eta^3$-cin)($\mu$-Cl)]$_2$ mixture.

**Table S6.** Optimisation of reaction conditions - Undivided cell.

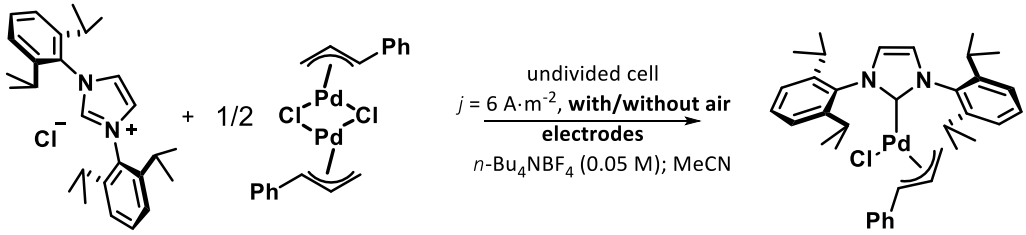


| Entry | Conditions | n (e), F/mol | Conv. Pd (Conv. Imid), % | Yield[a], % |
|---|---|---|---|---|
| 1[c] | C = A = Zn; air. atm. | 1.6 | 100 (75) | 53 |
| 2[c] | C = Zn; A = glassy carbon; air atm | 1.6 | 100 (53) | 46 |
| 3[c] | C = A = Zn; Ar atm. (gloxebox) | 1.6 | 100 (25) | 18[b] |
| 4[c] | C = A = Zn; continuous bubbling with air throughout the reaction | 1.6 | 100 (59) | 48 |

[a] Yield determined by NMR using 1,3,5-trimethoxybenzene as an internal standard. [b] Reaction accompanied by the formation of a substantial amount of Pd black which covered electrodes and precipitated. [c] Using [IPrH][Pd($\eta^3$-cin)$Cl_2$] instead of the IPr·HCl + ½ [Pd($\eta^3$-cin)($\mu$-Cl)]$_2$ reaction mixture.

**$H_2O_2$ qualitative analysis procedure**

Starch solution (1%) preparation: A slurry of soluble starch (0.5 g) in water (2 mL) was made which was poured into boiling water (25 mL). The resultant mixture was boiled for 5 minutes, diluted to 50 mL and allowed to cool.

A reagent solution was prepared by adding 60 µL of concentrated (95 %) sulfuric acid, 166 mg KI, and 0.77 mL 1 % starch solution to 10 mL degassed distilled water (solution **A**).

Then 1 mL of solution **A** was added to both reaction mixture after electrolysis (solution **B**) and to mimicked solution (solution **C**) (2.5 mL) containing 0.05 mmol of the target product [Pd($\eta^3$-cin)(Cl)(IPr)] and 0.05 M *n*-$Bu_4NBF_4$. Both solutions (**B** and **C**) were then degassed with Ar one more time to remove $O_2$ traces.

No colour change was observed for solution **C** whereas solution **B** rapidly turned dark blue/violet. Based on experimental results, we drew the conclusion, that the solution **B** contained an oxidant, which is presumably hydrogen peroxide, that oxidized KI in an acidic media, whereas the absence of colour change in case of the solution **C** suggests that there is no oxidant present.

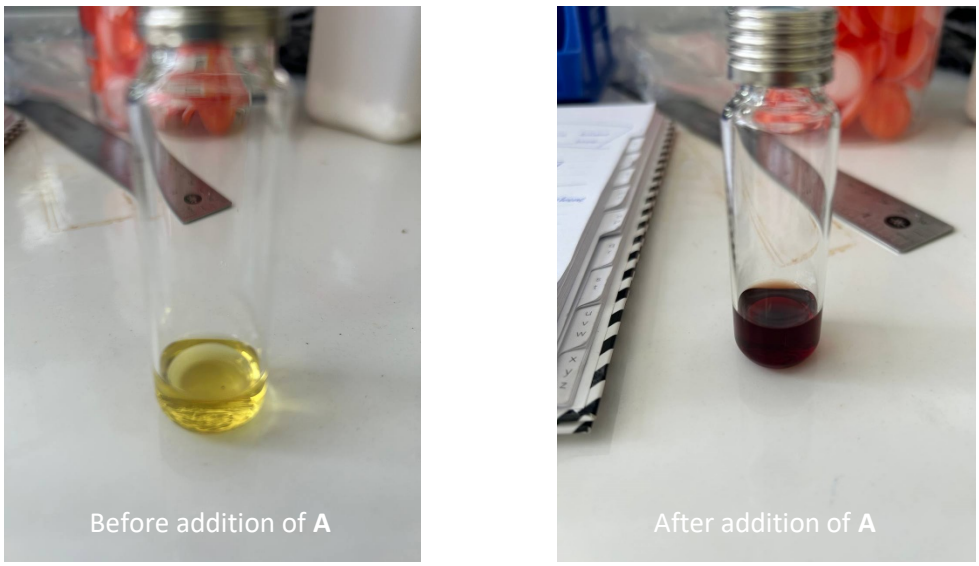


**Figure S13.** Test carried out on solution **B** -Before/After addition of solution **A**.

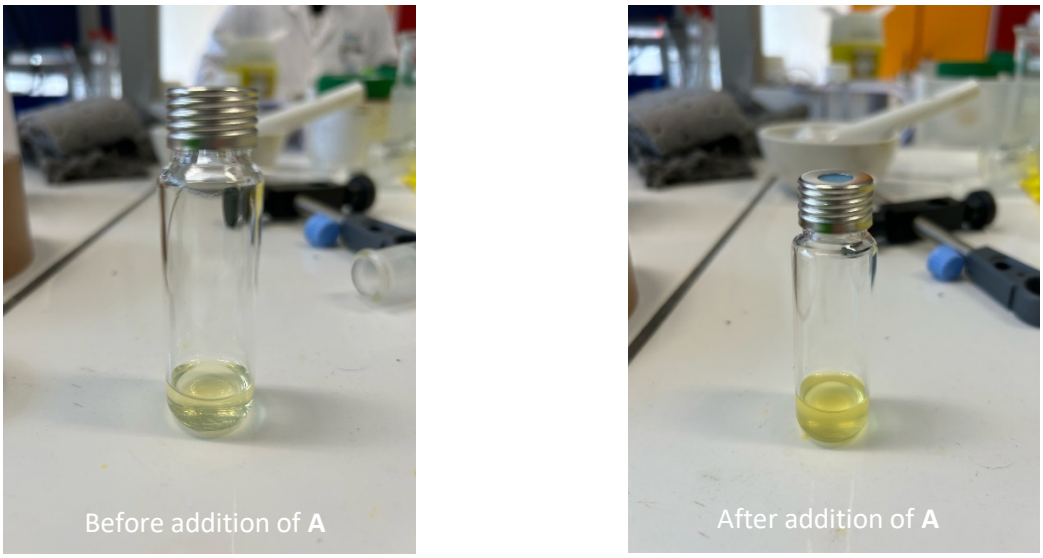


**Figure S14.** Test carried out on solution solution **C** - Before/After addition of solution **A**.

**Synthesis of [*n*-$Bu_4N$][Pd($\eta^3$-cin)$Cl_2$]**

*n*-$Bu_4NCl$ (30 mg, 0.108 mmol) and [Pd($\eta^3$-cin)(μ-Cl)]$_2$ (27.9 mg, 0.054 mmol) were dissolved in 2 ml of acetonitrile. Then the solvent was removed on a rotary evaporator, which yielded [*n*-$Bu_4N$][Pd($\eta^3$-cin)$Cl_2$] (57.9 mg) as an orange oil.

**$^1$H NMR (400 MHz, $CDCl_3$):** δ (ppm) = 7.48 – 7.42 (m, 2H, *o*-C$\underline{H}^{Ar}$), 7.21 – 7.14 (m, 3H, *m*(*p*)-C$\underline{H}^{Ar}$), 5.62 (ddd, *J* = 11.8, 11.2, 6.8 Hz, 1H, cin PhCH=C$\underline{H}$), 4.40 (d, *J* = 11.2 Hz, 1H, cin PhC$\underline{H}$=CH), 3.85 (d, *J* = 6.8 Hz, 1H, cin C$\underline{H}_2$ $H_{syn}$), 3.38 – 3.11 (m, 8H, N-C$\underline{H}_2$-), 2.88 (d, *J* = 11.8 Hz, 1H, cin C$\underline{H}_2$ $H_{anti}$), 1.58 (m, 8H, N-$CH_2$-C$\underline{H}_2$-), 1.37 (sextet, *J* = 7.4 Hz, 8H, N-$(CH_2)_2$-C$\underline{H}_2$-), 0.93 (t, *J* = 7.4 Hz, 12H, N-$(CH_2)_3$-C$\underline{H}_3$).

The compound could not be precipitated, that is obtained in a solid state, and thus was used in the form of a MeCN solution for the corresponding CV spectrum recording (Fig. S4). The formation of the palladate is clear from the comparison of NMR peaks chemical shift of the product and starting materials (see below).

**General procedure for the electrochemical preparation of Pd complexes**

The cathodic compartment of a split electrochemical cell was loaded with NHC·HCl (0.05 mmol), [Pd($\eta^3$-cin)($\mu$-Cl)]$_2$ or [Pd($\eta^3$-allyl)($\mu$-Cl)]$_2$ (0.025 mmol), and *n*-$Bu_4NBF_4$ (0.125 mmol; 41.1 mg), whereas the anodic chamber was loaded with $^n$$Bu_4NBF_4$ (0.125 mmol; 41.1 mg). Acetonitrile (2.5 mL) was added to each compartment. An anode and a cathode (Zn [8 x 52.5 x 2 mm]; $S_{immersed}$ = 4.2 cm$^2$) were immersed into the solution in both compartments. Constant current electrolysis (*I* = 2.5 mA) was carried out at room temperature with the reaction mixture being constantly stirred. As reaction goes along the reaction mixture steadily turns paler changing from yellow to beige/pale green. After completion of the reaction, the content of cathodic compartment was evaporated, transferred into a separation funnel containing EtOAc (15 mL) and washed 3 times with water (3 x 15 mL) portions. The organic phase was dried over $MgSO_4$ and filtered. The solvent was removed on a rotary evaporator. Pentane (5 mL) was added and the suspension was subjected to sonication (10-15 min). The product was collected by filtration and washed with hexane (5 mL).

**Synthesis of [Pd($\eta^3$-cin)(Cl)(IPr)] (1)**

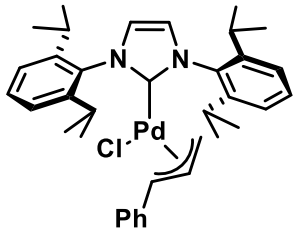


Following the general procedure with IPr·HCl (0.05 mmol; 21.3 mg) and [Pd($\eta^3$-cin)(μ-Cl)]$_2$ (0.025 mmol, 13.0 mg), [Pd($\eta^3$-cin)(Cl)(IPr)] was obtained as a beige solid in 83 % yield (26.4 mg, 0.041 mmol).

**$^1$H NMR (300 MHz, $CDCl_3$):** δ (ppm) = 7.46 (t, *J* = 7.8 Hz, 2H, ArH), 7.29 (d, *J* = 7.8 Hz, 4H, ArH), 7.17 – 7.10 (m, 7H, cin ArH, NCH=CHN), 5.07 (dt, *J* = 12.9, 9.3 Hz, 1H, cin PhCH=CH), 4.33 (d, *J* = 12.7 Hz, 1H, cin PhCH=CH), 3.10 – 2.87 (m, 5H, cin $CH_2$ $H_{syn}$, CH-$CH_3$), 1.75 (d, *J* = 11.6 Hz, 1H, cin $CH_2$ $H_{anti}$), 1.44-1.31 (m, 12H, CH-$CH_3$), 1.13 (d, *J* = 6.8 Hz, 12H, CH-$CH_3$). The spectrum matches reported literature data.[7]

**Synthesis of [Pd($\eta^3$-allyl)(Cl)(IPr)] (2)**

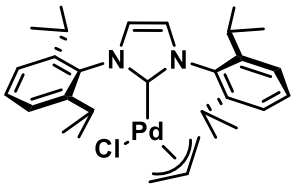

Following the general procedure with IPr·HCl (0.05 mmol; 21.3 mg) and [Pd($\eta^3$-allyl)(μ-Cl)]$_2$ (0.025 mmol, 9.1 mg) and acetone as a solvent, [Pd($\eta^3$-allyl)(Cl)(IPr)] was obtained as a pale yellow solid in 70 % yield (20.0 mg, 0.035 mmol).

**$^1$H NMR (300 MHz, $CDCl_3$):** δ (ppm) = 7.42 (t, *J* = 7.8 Hz, 2H, ArH), 7.31 – 7.23 (4H, ArH), 7.15 (s, 2H, NCH=CHN), 4.81 (tt, *J* = 13.7, 7.1 Hz, 1H, allyl $H_{meso}$), 3.89 (dd, *J* = 7.4, 2.3 Hz, 1H, allyl $H_{syn}$), 3.17 – 3.07 (m, 2H, CH-$CH_3$), 3.04 (d, *J* = 6.5 Hz, 1H, allyl $H_{syn}$), 3.17 – 3.07 (m, 2H, CH-$CH_3$), 2.90 – 2.80 (m, 2H, CH-$CH_3$), ), 2.77 (d, *J* = 13.5 Hz, 1H, allyl $H_{anti}$), 1.57 (d, *J* = 12.0 Hz, 1H, allyl $H_{anti}$),. 1.38 (d, *J* = 6.8 Hz, 6H, CH-C$H_3$), 1.33 (d, *J* = 6.8 Hz, 6H, CH-C$H_3$), 1.17 (d, *J* = 6.8 Hz, 6H, CH-C$H_3$), 1.08 (d, *J* = 6.9 Hz, 6H, CH-C$H_3$). The spectrum matches reported literature data. [8]

**Synthesis of [Pd($\eta^3$-cin)(Cl)(IMes)] (3)**

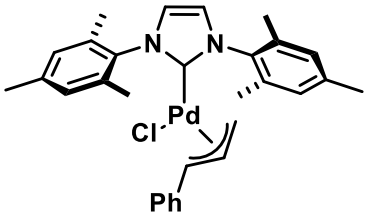

Following the general procedure with IMes·HCl (0.05 mmol; 17.0 mg) and [Pd($\eta^3$-cin)(μ-Cl)]$_2$ (0.025 mmol, 13.0 mg), [Pd($\eta^3$-cin)(Cl)(IMes)] was obtained as a beige solid in 80 % yield (22.4 mg, 0.040 mmol).

**$^1$H NMR (300 MHz, $CDCl_3$):** δ (ppm) = 7.13 (s, 4H, ArH), 7.09 (s, 2H, NCH=CHN), 7.03 – 6.95 (m, 5H, cin ArH), 5.16 (td, *J* = 12.4, 7.2 Hz, 1H, cin PhCH=CH), 4.34 (d, *J* = 12.4 Hz, 1H, cin PhCH=CH), 3.19 (d, *J* = 7.2 Hz, 1H, cin $CH_2$ $H_{syn}$), 2.35 (s, 6H, C$H_3$), 2.29 (br s, 1H, cin $CH_2$ $H_{anty}$), 2.24 (br s, 6H, C$H_3$), 2.19 (br s, 6H, C$H_3$). The spectrum matches reported literature data.[9]

**Synthesis of [Pd($\eta^3$-cin)(Cl)(SIPr)] (4)**

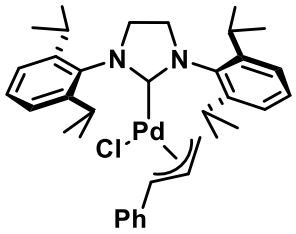


Following the general procedure with SIPr·HCl (0.05 mmol; 21.4 mg) and [Pd($\eta^3$-cin)(μ-Cl)]$_2$ (0.025 mmol, 13.0 mg), [Pd($\eta^3$-cin)(Cl)(SIPr)] was obtained as a pale yellow solid in 71 % yield (23 mg, 0.035 mmol).

**$^1$H NMR (300 MHz, $CDCl_3$):** δ (ppm) = 7.37 (t, *J* = 7.7 Hz, 2H, ArH), 7.24 (d, *J* = 7.7 Hz, 4H, ArH), 7.16 – 7.09 (m, 5H, cin ArH), 5.05 (td, *J* = 13.0, 9.2 Hz 1H, cin PhCH=CH), 4.32 (d, *J* = 13.0 Hz, 1H, cin PhCH=CH), 4.03 (s, 4H, $NCH_2CH_2N$), 3.43 (br s, 4 H, CH-$CH_3$), 2.88 (br s, 1H, cin $CH_2$ $H_{syn}$), 1.48-1.39 (m, 12H, CH-$CH_3$), 1.27 (d, *J* = 6.8 Hz, 12H, CH-$CH_3$), 1.27 – 1.23 (m, 1H, cin $CH_2$ $H_{anti}$). The spectrum matches reported literature data.[10]

**Synthesis of [Pd($\eta^3$-cin)(Cl)(SIMes)] (5)**

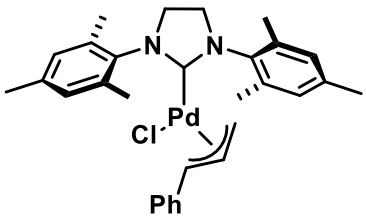


Following the general procedure with SIMes·HCl (0.05 mmol; 17.1 mg) and [Pd($\eta^3$-cin)(μ-Cl)]$_2$ (0.025 mmol, 13.0 mg), [Pd($\eta^3$-cin)(Cl)(SIMes)] was obtained as a yellowish solid in 74 % yield (20.8 mg, 0.037 mmol).

**$^1$H NMR (300 MHz, $CDCl_3$):** δ (ppm) = 7.15 – 7.01 (m, 5H, cin ArH), 6.96 (s, 2H, ArH), 6.94 (s, 2H, ArH), 5.08 (td, *J* = 12.5, 6.9 Hz, 1H, cin PhCH=CH), 4.26 (d, *J* = 12.5 Hz, 1H, cin PhCH=CH), 3.98 (s, 4H, $NCH_2CH_2N$), 3.27 (d, *J* = 6.9 Hz, 1H, cin $CH_2$ $H_{syn}$), 2.45 (s, 6H, $CH_3$), 2.41 (s, 6H, $CH_3$), 2.31 (s, 6H, $CH_3$), 1.92 (d, *J* = 12.5 Hz, 1H, cin $CH_2$ $H_{anti}$). The spectrum matches reported literature data.[7]

**Synthesis of [Pd($\eta^3$-cin)(Cl)(SIPr(OMe))] (6)**

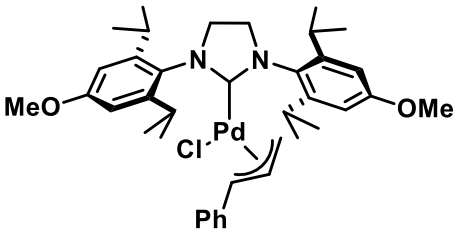


Following the general procedure with SIPr(OMe)·HCl (0.05 mmol; 24.4 mg) and [Pd($\eta^3$-cin)(μ-Cl)]$_2$ (0.025 mmol, 13.0 mg), [Pd($\eta^3$-cin)(Cl)(SIPr(OMe))] was obtained as a yellowish solid in 66 % yield (23.3 mg, 0.033 mmol).

**$^1$H NMR (300 MHz, $CDCl_3$):** δ (ppm) = 7.18 – 7.09 (m, 5H, cin Ar<u>H</u>), 6.73 (s, 4H, Ar<u>H</u>), 5.09 (dt, *J* = 12.9, 9.2 Hz, 1H, cin PhCH=C<u>H</u>), 4.35 (d, *J* = 13.0 Hz, 1H, cin PhC<u>H</u>=CH), 3.96 (s, 4H, NC<u>H$_2$</u>C<u>H$_2$</u>N), 3.85 (s, 6H, OC<u>H$_3$</u>), 3.40 (br s, 4 H, C<u>H</u>-CH$_3$), 2.90 (br s, 1H, cin C<u>H$_2$</u> H$_{syn}$), 1.62 (br s, 1H, cin C<u>H$_2$</u> H$_{anti}$), 1.40 (d, *J* = 6.7 Hz, 12H, CH-C<u>H$_3$</u>), 1.25 (d, *J* = 6.7 Hz, 12H, CH-C<u>H$_3$</u>).

**$^{13}$C NMR (100 MHz, $CDCl_3$):** δ (ppm) = 213.0 (N<u>C</u>N), 159.6 (<u>C</u>-OCH$_3$), 148.7 (*o*-CH$^{ArOMe}$), 137.8 (*i*-CH$^{ArOMe}$), 129.8 (*i*-C$^{Ar}$), 128.4 (*o*-CH$^{Ar}$), 127.4 (*m*-CH$^{Ar}$), 126.8 (*p*-CH$^{Ar}$), 109.6 (*m*-CH$^{ArOMe}$), 109.2 (PhCH=<u>C</u>H-CH$_2$), 91.9 (Ph<u>C</u>H=CH-CH$_2$), 55.3 (O<u>C</u>H$_3$), 54.2(N<u>C</u>H$_2$<u>C</u>H$_2$N), 46.0 (cin PhCH=CH-<u>C</u>H$_2$), 28.9 (<u>C</u>H-CH$_3$), 26.7 (CH-<u>C</u>H$_3$).

**Elemental Analysis**: Calculated: C 64.31, H 7.24, N 3.95. Found: C 64.08, H 7.41, N 3.85.

**Synthesis of [Pd($\eta^3$-cin)(Cl)(IPr$^{(Cl)}$)] (7)**

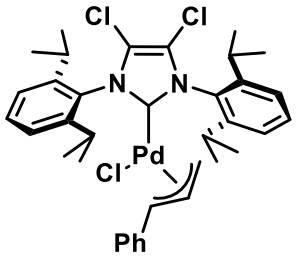


Following the general procedure with IPr$^{(Cl)}$·HCl (0.05 mmol; 24.7 mg) and [Pd($\eta^3$-cin)(μ-Cl)]$_2$ (0.025 mmol, 13.0 mg), [Pd($\eta^3$-cin)(Cl)(IPr$^{(Cl)}$)] was obtained as a beige solid in 67 % yield (24.1 mg, 0.033 mmol).

**$^1$H NMR (300 MHz, $CDCl_3$):** δ (ppm) = 7.52 (t, *J* = 7.8 Hz, 2H, Ar<u>H</u>), 7.33 (d, *J* = 7.8 Hz, 4H, Ar<u>H</u>), 7.17 – 7.10 (m, 5H, cin Ar<u>H</u>), 5.07 (dt, *J* = 12.6, 9.3 Hz, 1H, cin PhCH=C<u>H</u>), 4.34 (d, *J* = 12.6 Hz, 1H, cin PhC<u>H</u>=CH), 3.22 – 3.01 (m, 1H, cin C<u>H$_2$</u> H$_{syn}$), 3.01 – 2.81 (m, 4H, C<u>H</u>-CH$_3$), 1.92 – 1.76 (m, 1H, cin C<u>H$_2$</u> H$_{anti}$), 1.37 (br s, 12H, CH-C<u>H$_3$</u>), 1.20 (d, *J* = 6.9 Hz, 12H, CH-C<u>H$_3$</u>). The spectrum matches reported literature data.[11]

**Synthesis of [Pd($\eta^3$-cin)(Cl)(BIAN-IMes)] (8)**

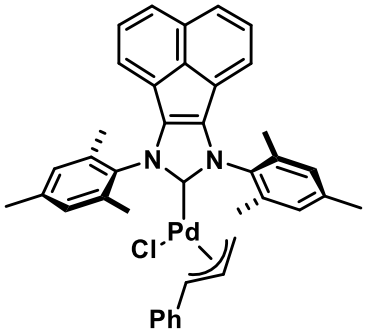


Following the general procedure with BIAN-IMes·HCl (0.05 mmol; 24.7 mg) and [Pd($\eta^3$-cin)(μ-Cl)]$_2$ (0.025 mmol, 13.0 mg), [Pd($\eta^3$-cin)(Cl)(BIAN-IMes)] was obtained as a yellow solid in 79 % yield (27.0 mg, 0.039 mmol).

**$^1$H NMR (300 MHz, $CDCl_3$):** δ (ppm) = 7.73 (d, *J* = 8.2 Hz, 2H, ArH), 7.38 (dd, *J* = 8.2, 7.0 Hz, 2H, ArH), 7.22 – 7.13 (m, 5H, cin ArH), 7.09 (br s, 2H, ArH), 7.07 (br s, 2H, ArH), 6.99 (d, *J* = 6.9 Hz, 2H, ArH), 5.24 (dt, *J* = 12.5, 9.6 Hz, 1H, cin PhCH=CH), 4.44 (d, *J* = 12.5 Hz, 1H, cin PhCH=CH), 3.28 (d, *J* = 6.8 Hz, 1H, cin $CH_2$ $H_{syn}$), 2.42 (s, 6H, $CH_3$), 2.34 (s, 6H, $CH_3$), 2.29 (s, 6H, $CH_3$), 2.05 (d, *J* = 11.9 Hz, 1H, cin $CH_2$ $H_{anti}$).

**$^{13}$C NMR (100 MHz, $CDCl_3$):** δ (ppm) = 189.4 (NCN), 139.1 ($C^{Ar}$), 138.9 ($C^{Ar}$), 138.3 ($C^{Ar}$), 135.5 ($C^{Ar}$), 135.4 ($C^{Ar}$), 134.6 ($C^{Ar}$), 129.7 ($C^{Ph}$), 129.5 ($C^{Ar}$), 128.4 ($C^{Ph}$), 127.9 ($C^{Ar}$), 127.7 ($C^{Ar}$), 127.5 ($C^{Ph}$), 126.8 ($C^{Ph}$), 126.0 ($C^{Ar}$), 120.6 ($C^{Ar}$), 109.4 (PhCH=CH-$CH_2$), 90.3 (PhCH=CH-$CH_2$), 46.7 (cin PhCH=CH-$CH_2$), 21.4 (-$CH_3$), 18.6 (-$CH_3$), 18.6 (-$CH_3$).

**Elemental Analysis**: Calculated: C 69.87, H 5.42, N 4.07. Found: C 69.60, H 5.53, N 4.46.

## NMR spectra of compounds

*[Pd(η³-cin)(Cl)(IPr)] (**1**) – ¹H NMR spectrum*

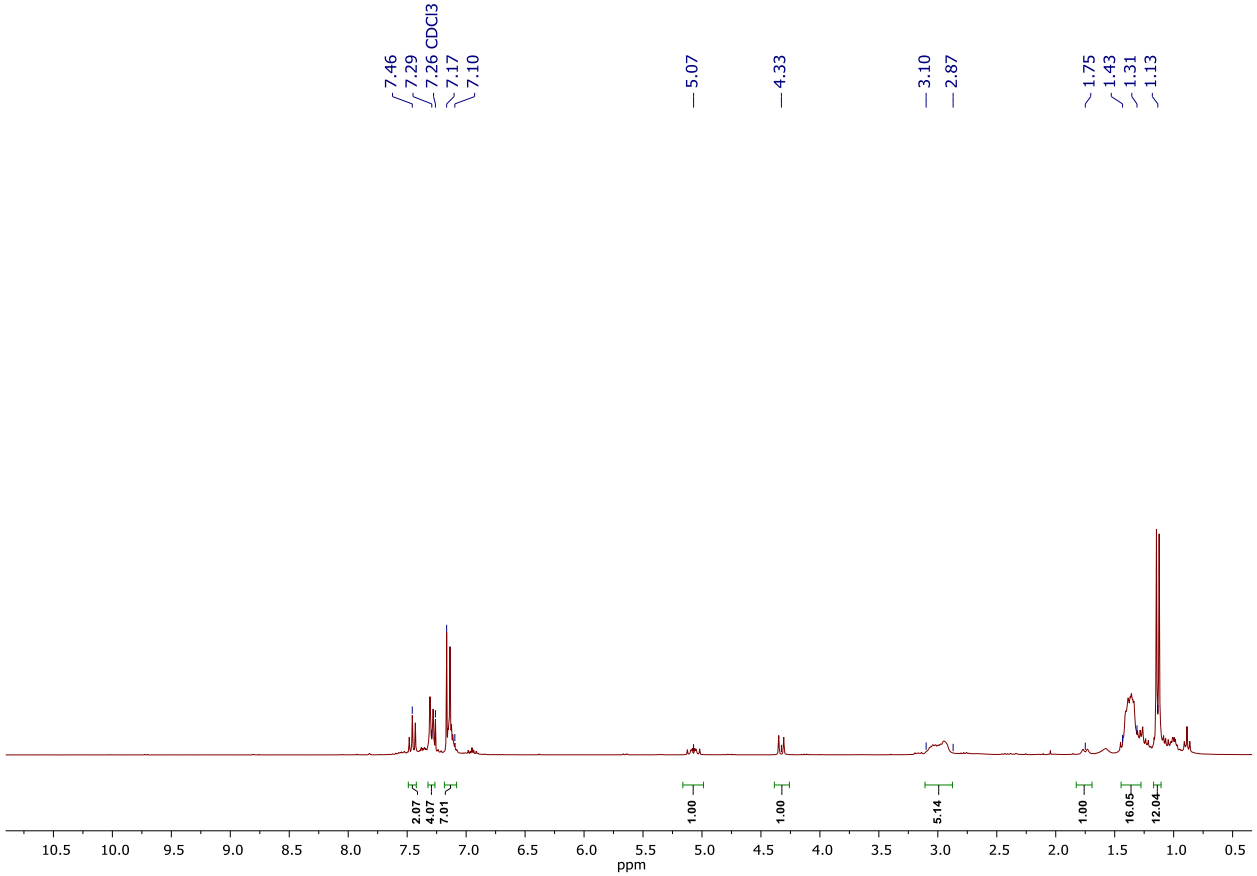


*[Pd(η³-allyl)(Cl)(IPr)] (**2**) – ¹H NMR spectrum*

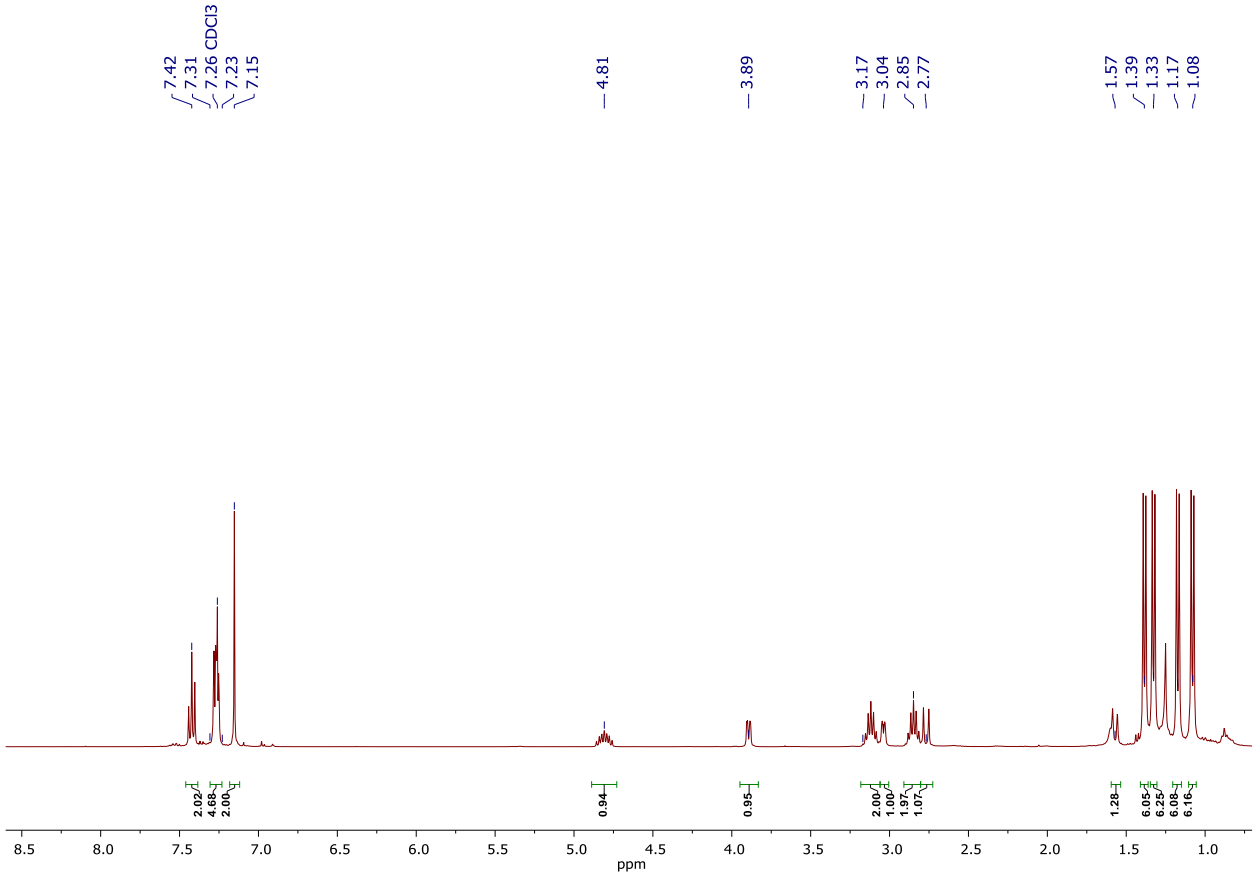

*[Pd(η³-cin)(Cl)(IMes)] (**3**) – ¹H NMR spectrum*

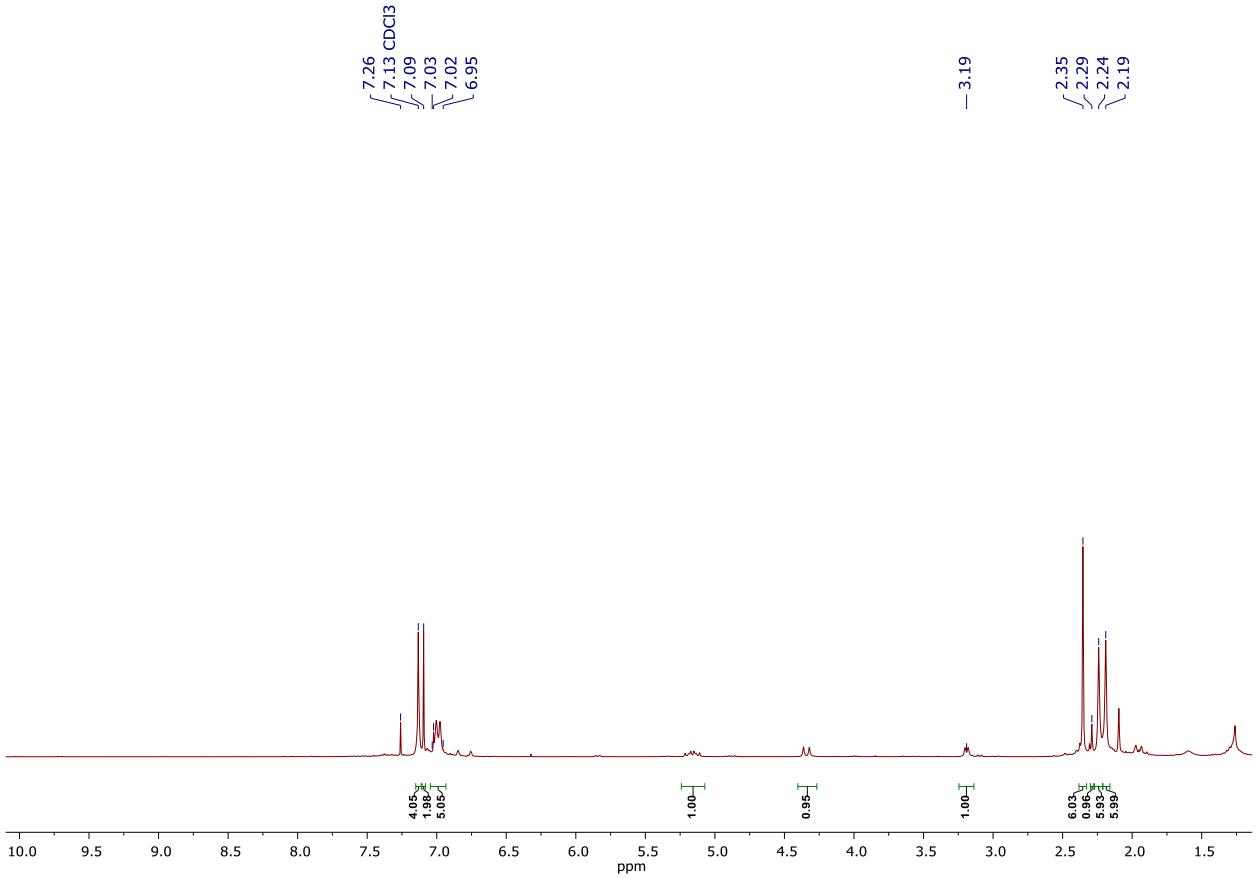


*[Pd(η³-cin)(Cl)(SIPr)] (**4**) – ¹H NMR spectrum*

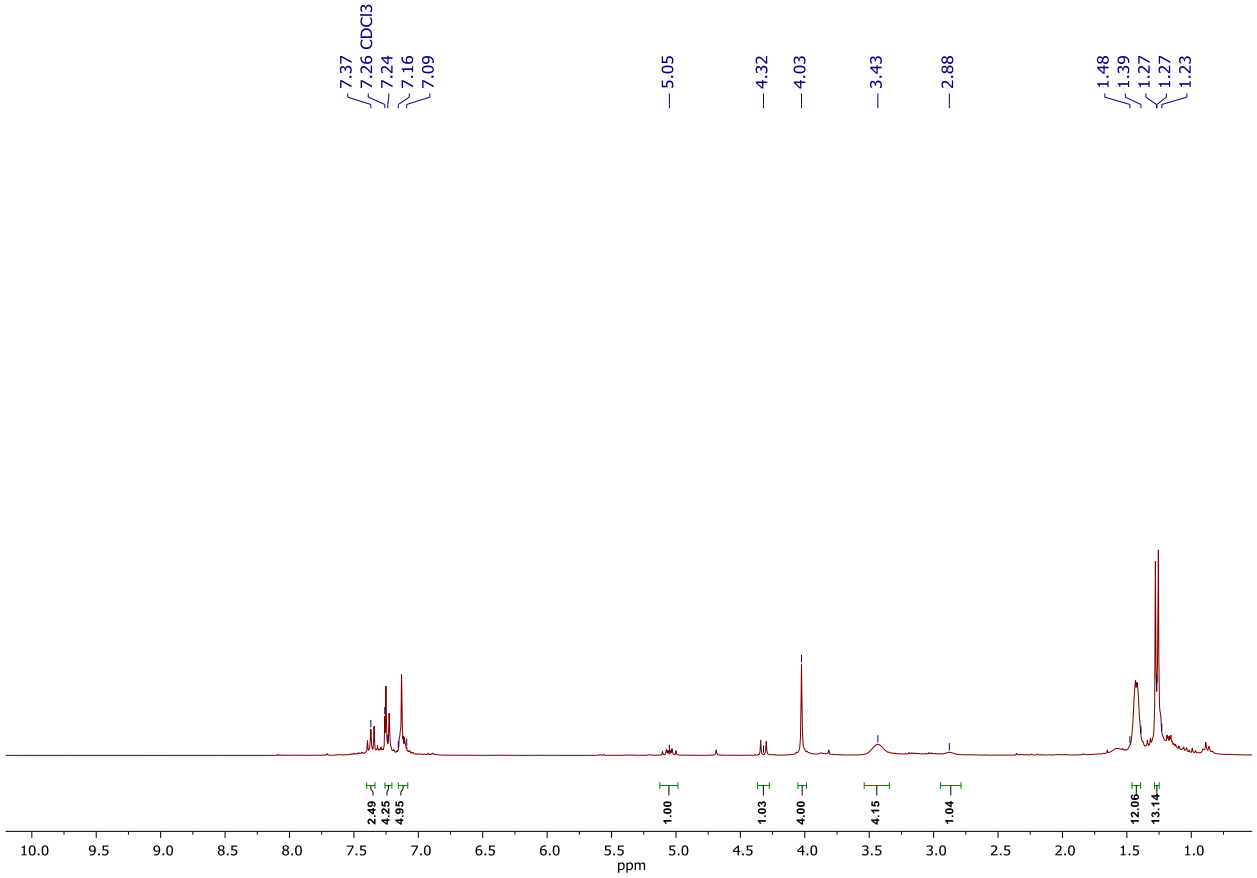

*[Pd(η³-cin)(Cl)(SIMes)] (**5**) – ¹H NMR spectrum*

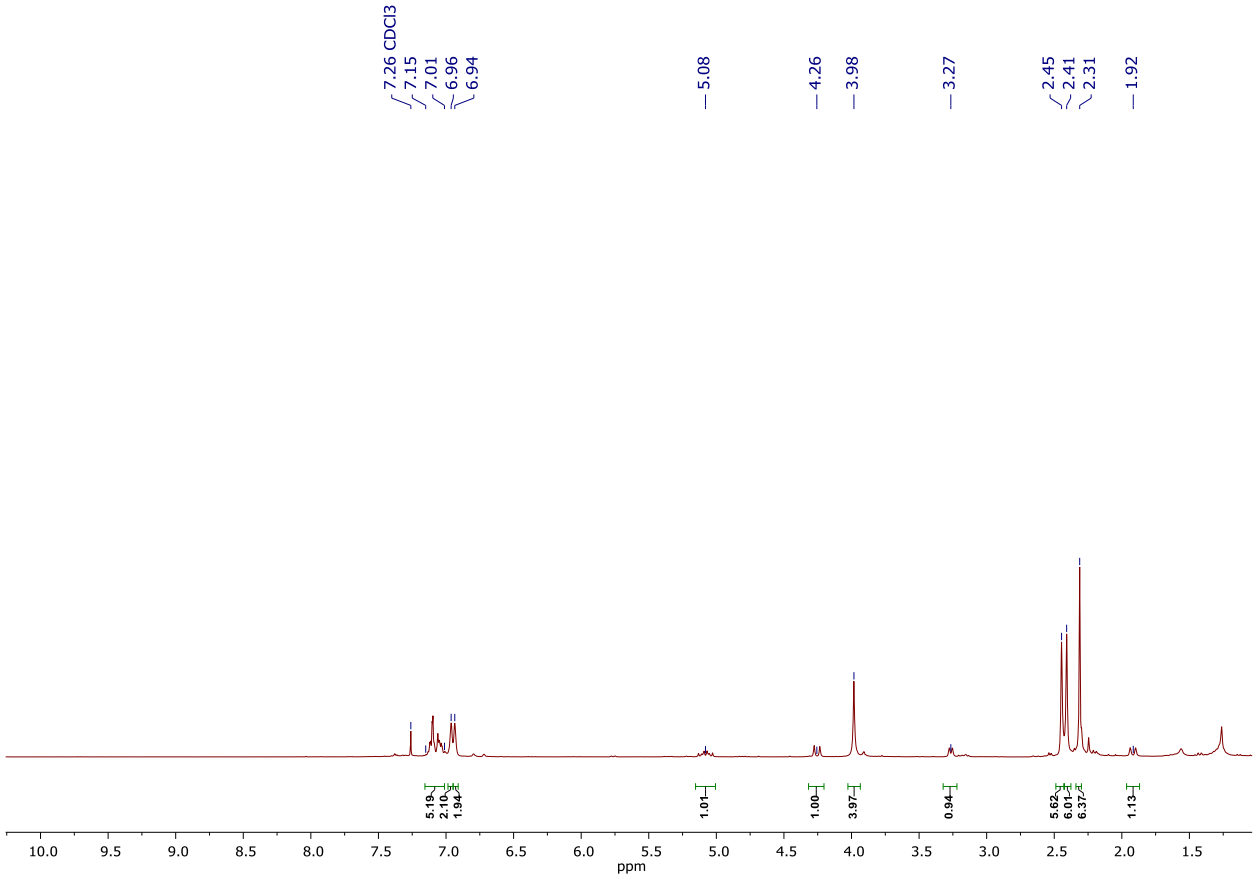

*[Pd(η³-cin)(Cl)(SIPr(OMe))] (**6**) – ¹H NMR spectrum*

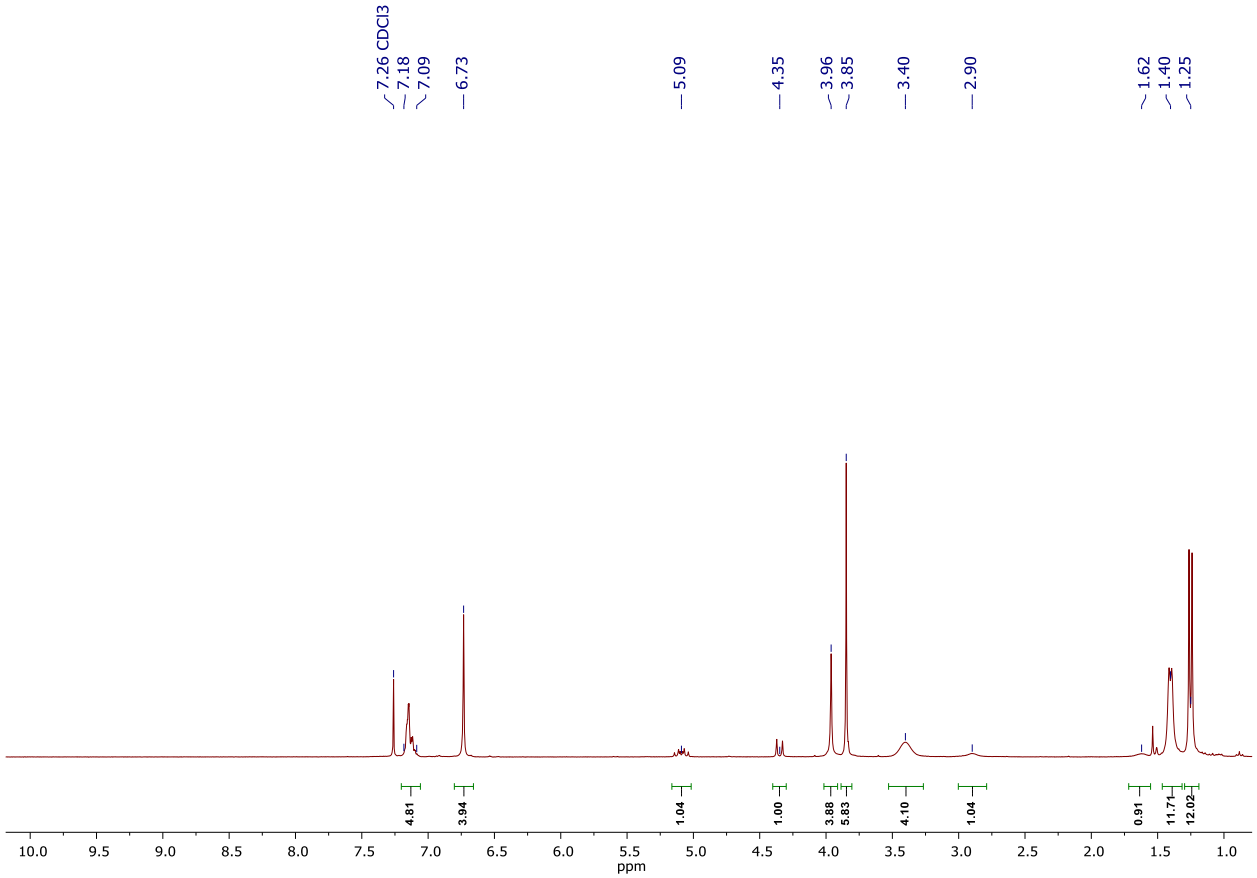


*[Pd(η³-cin)(Cl)(SIPr(OMe))] (**6**) – ¹³C {¹H} NMR spectrum*

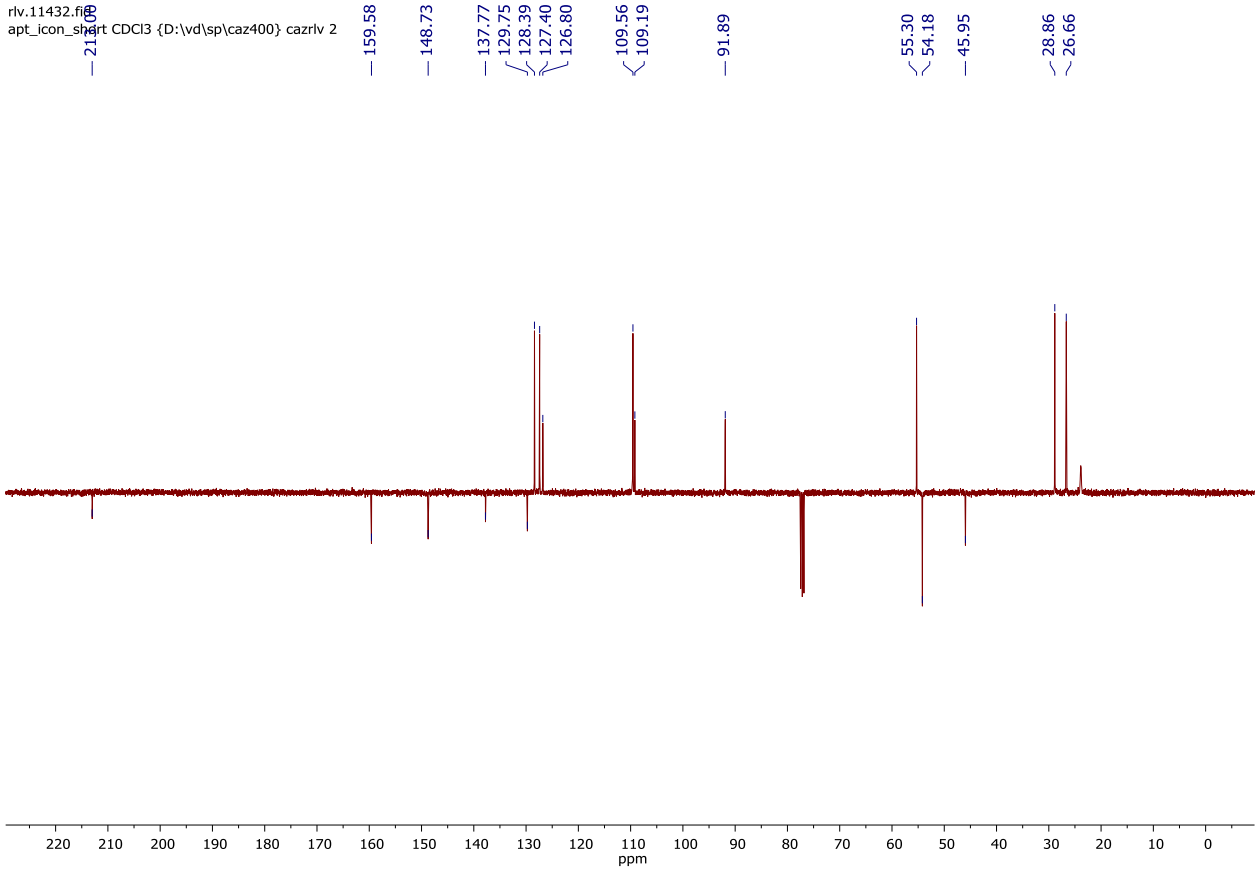

*[Pd(η³-cin)(Cl)(IPr$^{(Cl)}$)] (**7**) – $^{1}$H NMR spectrum*

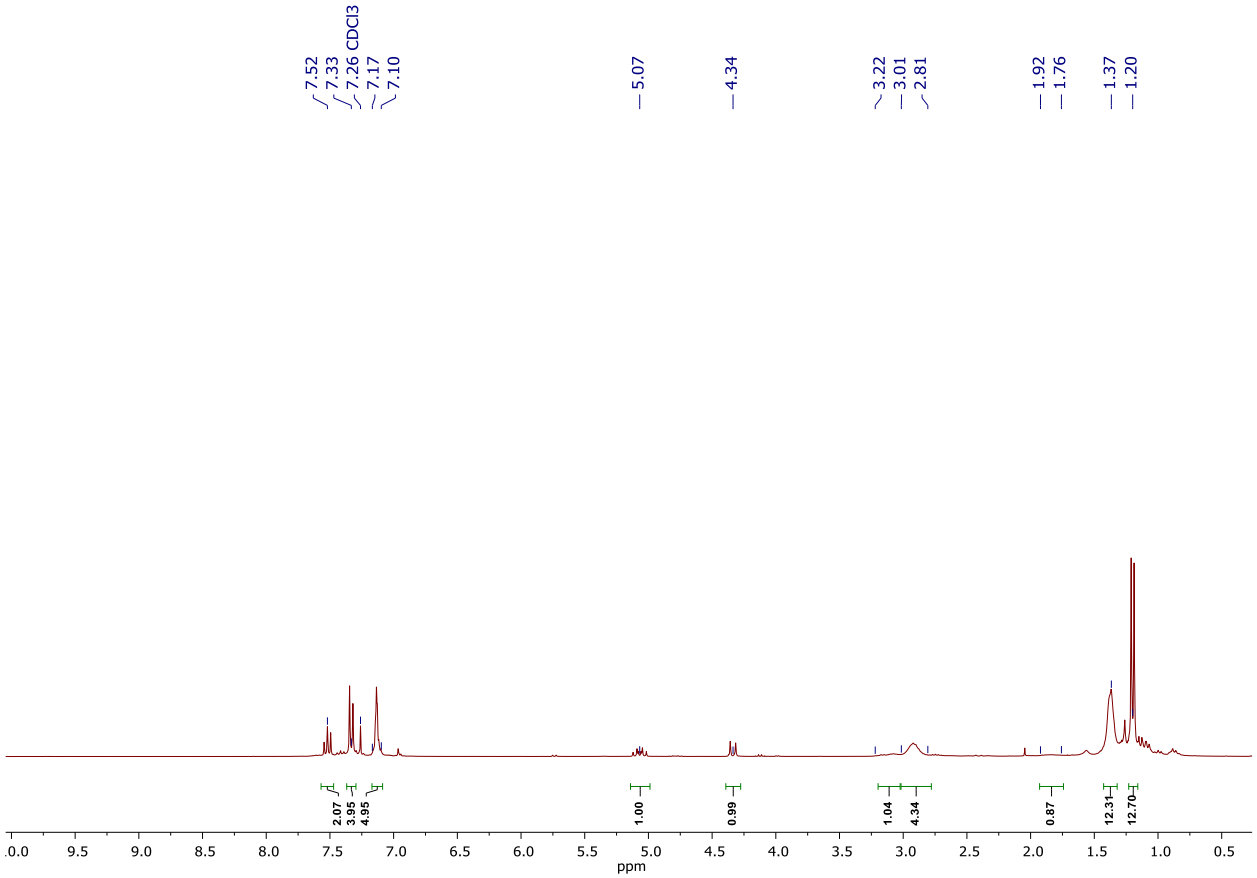

*[Pd(η³-cin)(Cl)(BIAN-IMes)] (**8**) – ¹H NMR spectrum*

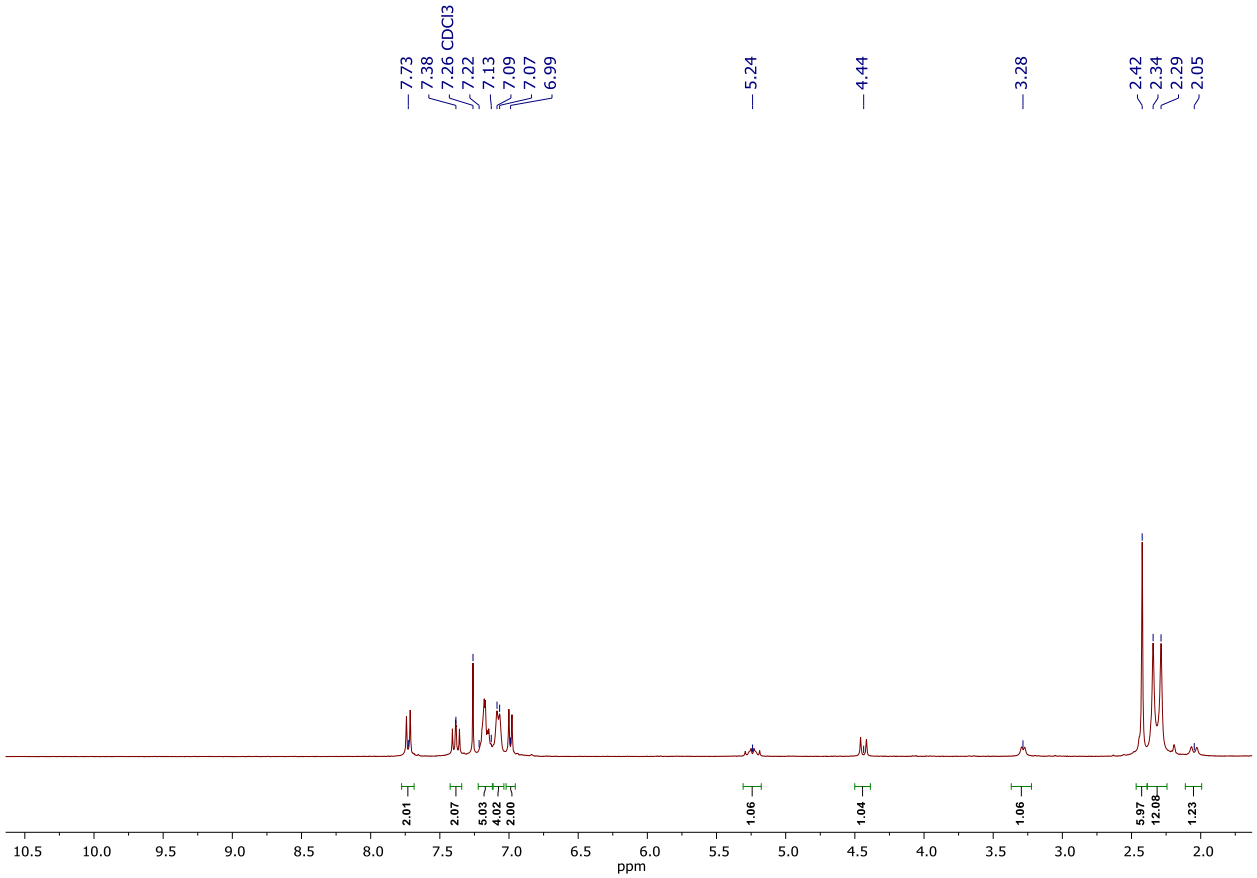


*[Pd(η³-cin)(Cl)(BIAN-IMes)] (**8**) – ¹³C {¹H} NMR spectrum*

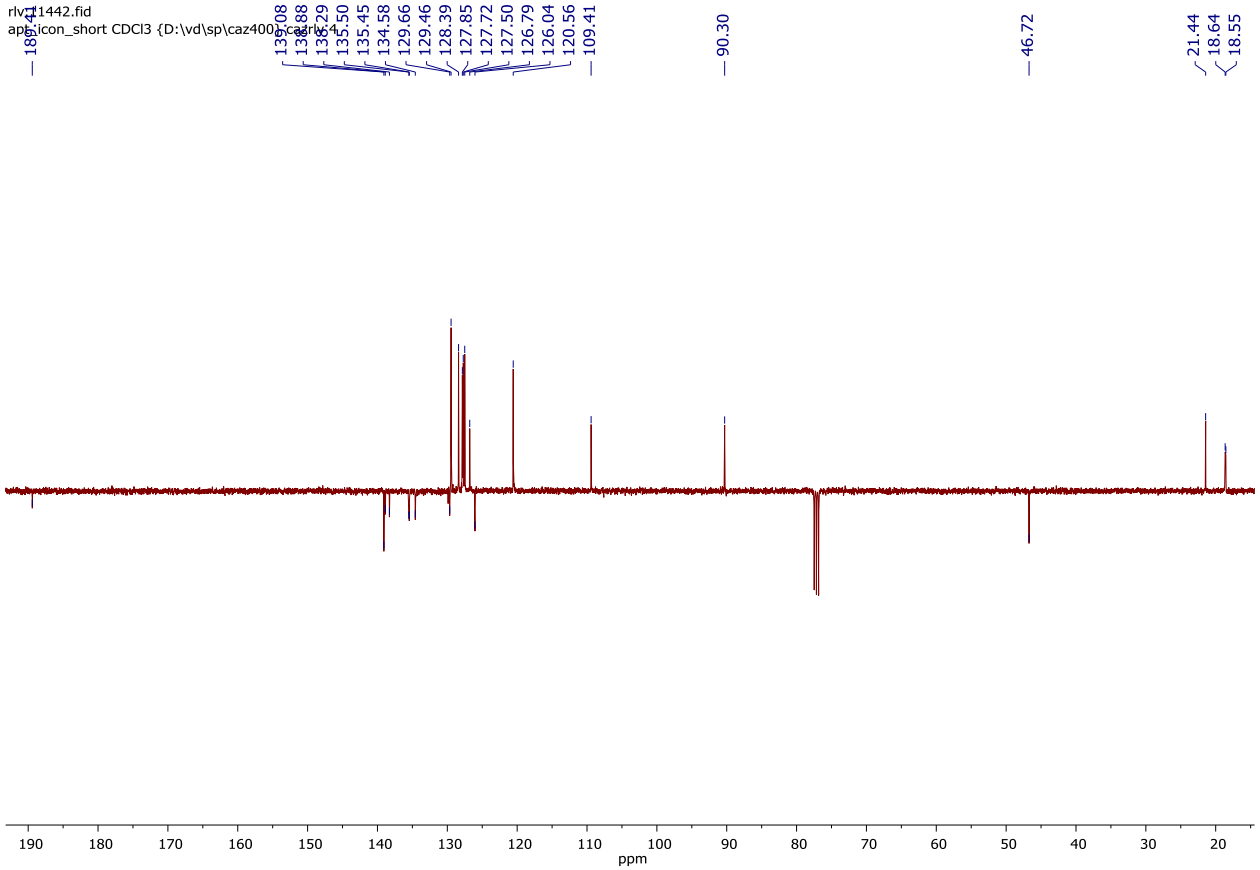

*[n-Bu$_4$N][Pd(η$^3$-cin)Cl$_2$] – $^1$H NMR spectrum*

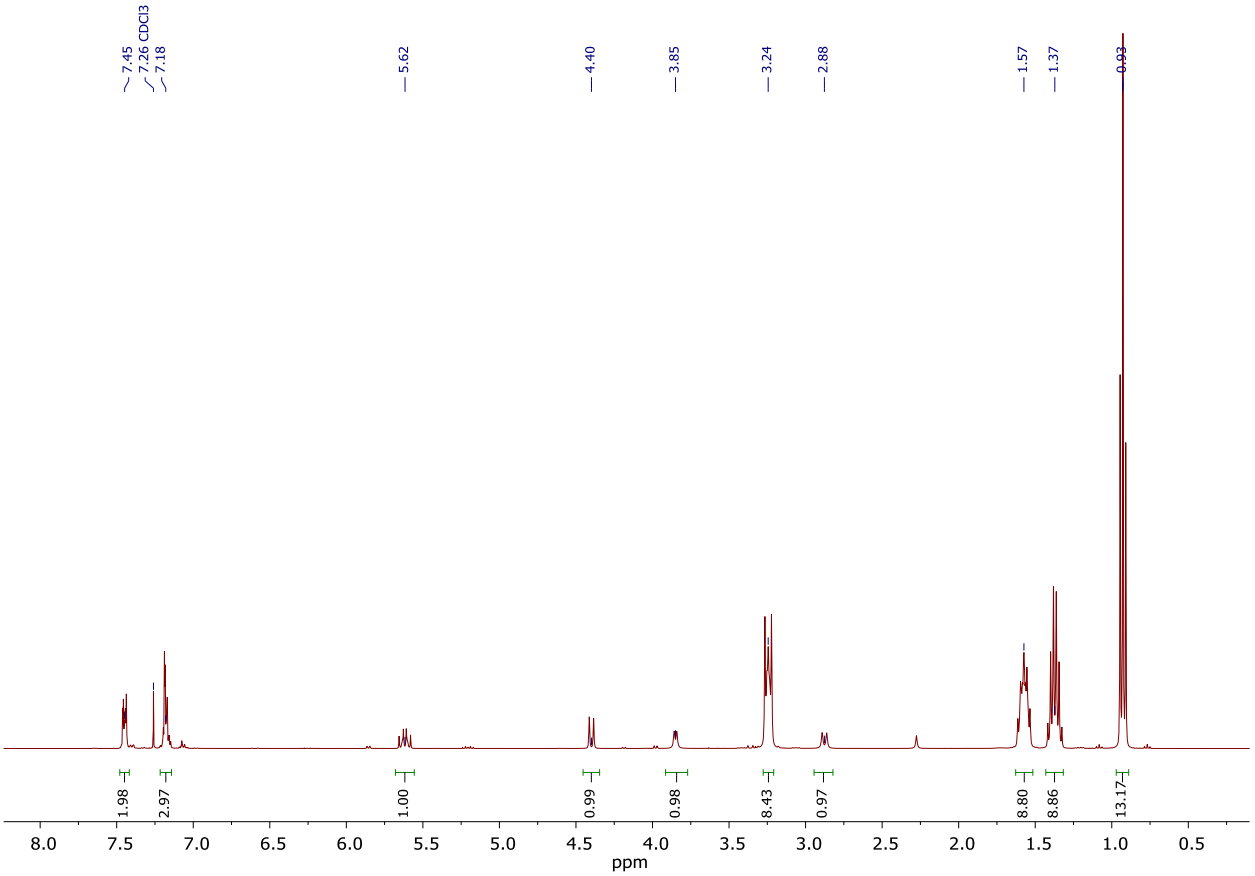


*Superimposition of the NMR spectra of n-Bu$_4$NCl, [Pd(η$^3$-cin)(μ-Cl)]$_2$, [n-Bu$_4$N][Pd(η$^3$-cin)Cl$_2$]*

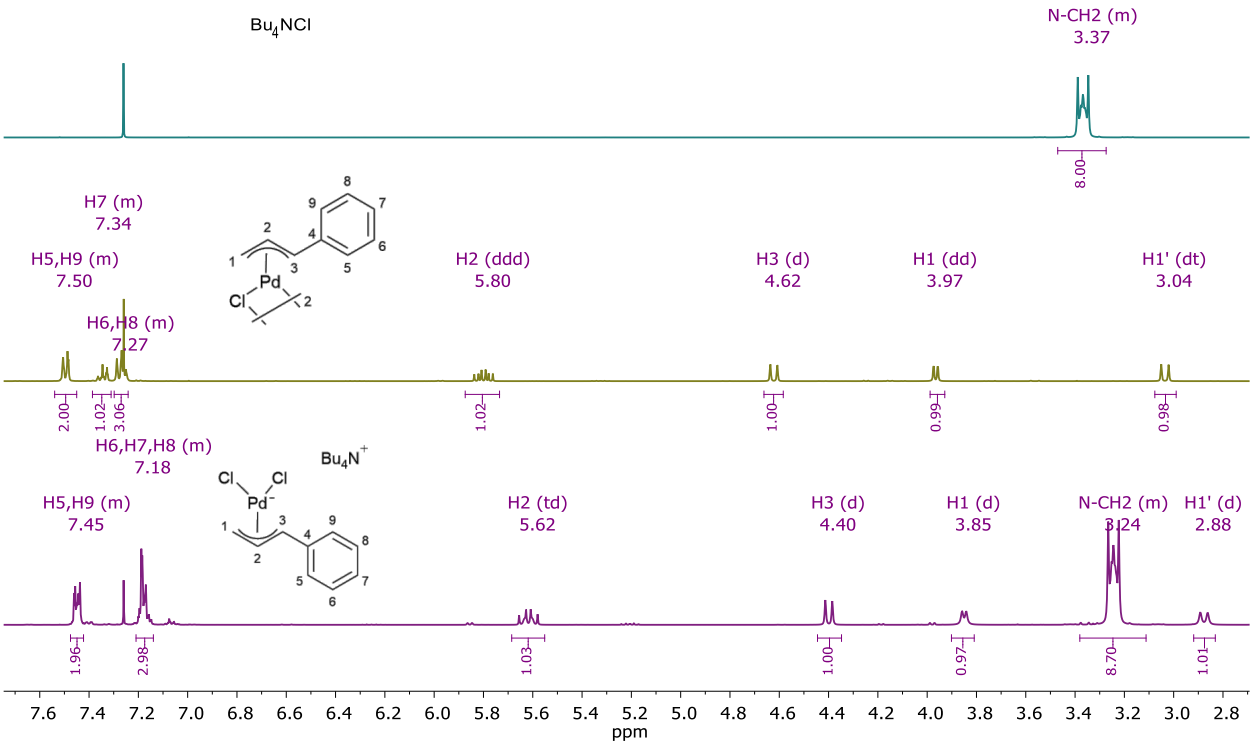

## References


1 X. Bantreil and S. P. Nolan, *Nat. Protoc.*, 2011, **6**, 69–77.
2 S. C. Gadekar, V. Dhayalan, A. Nandi, I. L. Zak, M. S. Mizrachi, S. Kozuch, and A. Milo, *ACS Catal.*, 2021, **11**, 14561-14569
3 S. Gaillard, A. M. Z. Slawin, A. T. Bonura, E. D. Stevens and S. P. Nolan, *Organometallics*, 2010, **29**, 394–402.
4 T. Tu, Z. Sun, W. Fang, M. Xu, and Y. Zhou, *Org. Lett.*, 2012, **14**, 4250-4253
5 S. Meiries and S. P. Nolan, *Synlett*, 2014, **25**, 393-398
6 V. V. Pavlishchuk, A. W. Addison, *Inorg. Chem. Acta*, 2000, **298**, 97-102
7 C. M. Zinser, F. Nahra, M. Brill, R. E. Meadows, D. B. Cordes, A. M. Z. Slawin, S. P. Nolan and C. S. J. Cazin, *Chem. Commun.*, 2017, **53**, 7990–7993.
8 M. S. Viciu, O. Navarro, R. F. Germaneau, R. A. Kelly, W. Sommer, N. Marion, E. D. Stevens, L. Cavallo and S. P. Nolan, *Organometallics*, 2004, **23**, 1629–1635.
9 S. K. Furfari, M. R. Gyton, D. Twycross and M. L. Cole, *Chem. Commun.*, 2015, **51**, 74–76.
10 G. Pisanò and C. S. J. Cazin, *ACS Sustain. Chem. Eng.*, 2021, **9**, 9625–9631.
11 F. Izquierdo, C. Zinser, Y. Minenkov, D. B. Cordes, A. M. Z. Slawin, L. Cavallo, F. Nahra, C. S. J. Cazin and S. P. Nolan, *ChemCatChem*, 2018, **10**, 601–611.